Preparation Methods for Large-Area Perovskite Solar Cells

Subjects: Materials Science, Coatings & Films | Energy & Fuels

Contributor: Melvin Mashingaidze, Shindume Lomboleni Hamukwaya, Huiying Hao, Jingjing Dong, JIE XING, Hao Liu

Solar energy is one of the most encouraging, abundant, green, and renewable sources for decreasing or even replacing traditional energy in the future. The energy provided by the sun in one hour is sufficient to supply the Earth's needs for an entire year. The recent rapid development in perovskite solar cells (PSCs) has led to significant research interest due to their notable photovoltaic performance, currently exceeding 25% power conversion efficiency for small-area PSCs. The materials used to fabricate PSCs dominate the current photovoltaic market, especially with the rapid increase in efficiency and performance.

Keywords: perovskite solar cells ; power conversion efficiency ; large-area perovskite films ; preparation and fabrication methods ; scalable ; quality and stability ; building-integrated photovoltaics

1. Introduction

Fossil fuels must be replaced by clean and renewable energy in order to reduce environmental pollution and meet an increase in global energy demands [1][2][3][4]. Solar energy is one of the most encouraging, abundant, green, and renewable sources for decreasing or even replacing traditional energy in the future. The energy provided by the sun in one hour is sufficient to supply the Earth's needs for an entire year [5].

Various innovative photovoltaic technologies have been developed to capture and convert solar energy into electricity, but affordable solar cells with high power conversion efficiency are needed. One of the frontrunner technologies uses inorganic and organic hybrid compounds (CH_3NH_3-PbX_3, X = I, Br, Cl) with the crystal structure of perovskite. Photovoltaic solar cells utilizing such light absorbers are called perovskite solar cells (PSCs). Some of the PSCs' favorable attributes compared to conventional solar cells such as the silicon-based rigid modules include ease of fabrication [6], diversity in device architectures [7], small energy band gaps, high carrier mobility [8], panchromatic sunlight absorption, superior carrier diffusion length, and long carrier lifetimes [7][9]. Unlike silicon, which only absorbs light near the red end of the visible light spectrum, perovskites can be tuned to absorb different wavelengths (https://www.technologyreview.com/2021/06/29/1027451/perovskite-solar-panels-hype-commercial-debut, accessed on 8 February 2022). However, PSCs tend to display poor long-term stability due to the natural instability of the active perovskite layer. The lifespan of PSCs is severely reduced by exposure to water, heat, oxygen, and light (https://resources.system-analysis.cadence.com/blog/msa2021-the-pros-and-cons-of-halide-perovskite-solar-panels, accessed on 8 February 2022). The power conversion efficiency of PSCs is generally lower than for comparable conventional silicon solar cells and drops with increasing size, which is a huge disadvantage for commercialization efforts. PSC power conversion efficiency is also dependent on the quality of the perovskite layer, which in turn is dependent on the synthesis method deployed. This leads to wide variability in reported PSC performance, further compounding the PSCs' commercialization challenge.

The reader is referred to the works of [10][11][12][13] for the structures (**Figure 1**) and characteristics of PSCs, the classifications of different materials used to enhance PSC performance, and the encapsulation materials and methods related to PSCs. A thorough analysis of PSCs' chemical stability is provided by [6][8][10][13], and the reader is advised to consider these works. The working principle of PSC architecture is as follows: the perovskite layer absorbs the incident light, and produces electrons and holes that are extracted and carried by electron transport materials (ETMs) and hole transport materials (HTMs), respectively, which are finally collected by electrodes, forming PSCs [11].

Figure 1 shows the archetypal PSC structures, including the mesoporous structure in **Figure 1**a, the planar heterojunction structure in **Figure 1**b, and the inverted planar heterojunction structure in **Figure 1**c. The PSCs with standard configurations have a transparent, conductive, oxide (TCO)/blocking layer ETL/perovskite absorber layer/HTL material/gold (Au). The perovskite absorption layer absorbs light and generates charges while light is incident on the PSC.

The photon energy creates pairs that diffuse and separate through electrons' and holes' selective contacts, as shown in **Figure 1**d [14]. Once electrons and holes are present at the cathode and anode, an external load can be powered by connecting a circuit to the cell.

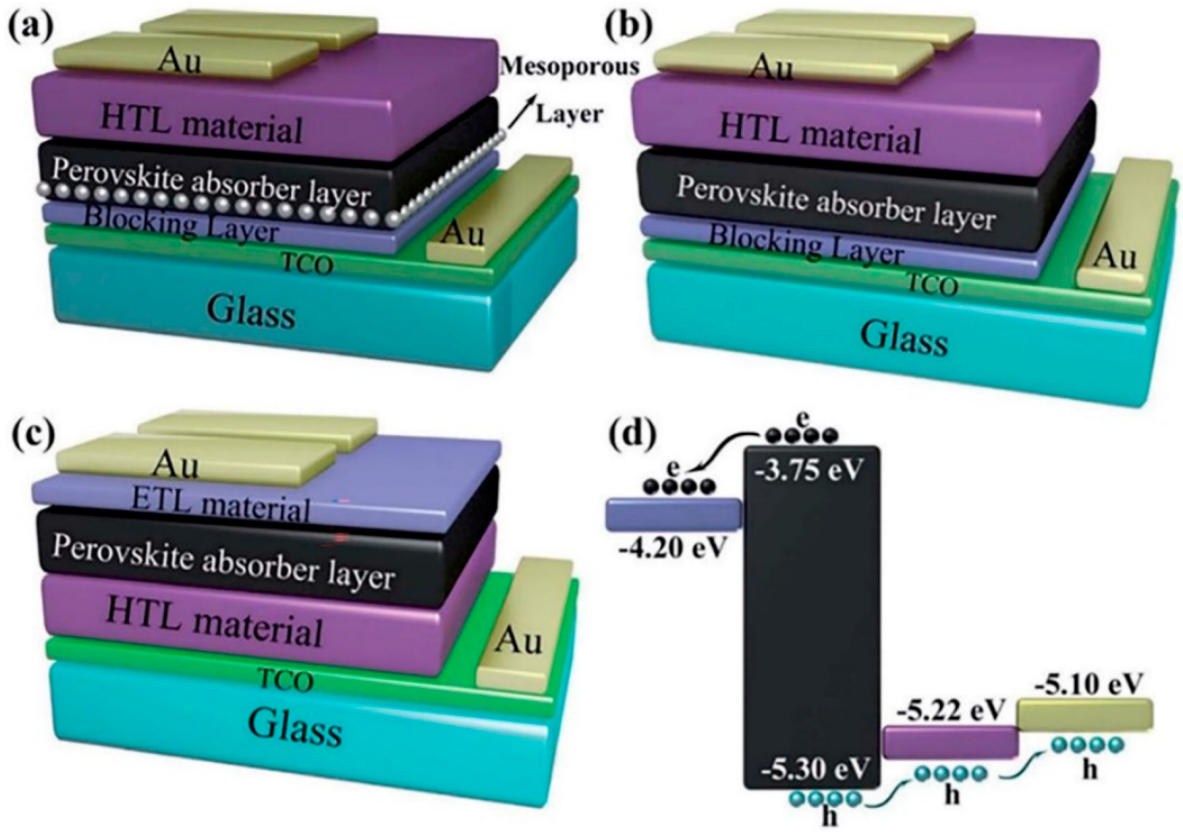

Figure 1. Structural configurations of perovskite solar cells: (**a**) mesoporous structure, (**b**) planar heterojunction structure, (**c**) inverted planar heterojunction structure, and (**d**) schematic diagram of electron and hole transportation [15].

The power conversion efficiency (PCE) of PSCs has reportedly risen from 3.8% to more than 25% over the past few years, surpassing established thin-film solar cells, such as CuInGaSeCdTe [16]. However, most high PCEs of PSCs have been reported for cells of small areas, from 0.04 to 0.2 cm^2 [17], and also for those manufactured by spin coating methods of areas ~0.1 cm^2 [18][19][20]. Few researchers have attempted to manufacture large-area solar cells. For PSCs to be evaluated for practical commercial applications, large-area cells (minimum active area > 1 cm^2) must be fabricated cost-effectively and achieve PCEs comparable to small-area cells.

Perovskite materials and preparation methods for large-area modules are essential for scalable deposition [21]. According to Kim et al., the two main challenges are currently preventing the synthesis of larger efficient PSCs and limiting the maximum device area to a few cm^2. These challenges include a severe decrease in perovskite film quality and uniformity for sizes greater than 1 cm^2 and the nearly linear rise in series resistance with cell area [22].

Wang et al. cited the drop in PSC efficiency accompanying the device's enlargement as a stumbling block to PSCs' commercial application and attribute the inefficiencies to each functional layer's imperfections in coverage, uniformity, and flatness, which arise from the solution processing method. Wang et al. questioned the high PCEs reported by some researchers for small-area PSCs since measurement errors normally increase as the active cell area decreases [12]. According to these authors, the second challenge for the commercialization of PSCs is poor stability, which worsens with the increase in cell size. The third challenge reported by Wang et al. is the cost of PSCs with PCEs being >20% higher, since they have to be manufactured from costly materials, such as Spiro-OMeTAD, Au, using costly vacuum deposition technology.

Despite the fact that spin coating has been extensively used to fabricate a dense and uniform perovskite film for PSC modules, film uniformity declines significantly as cell size grows, leading to very poor PCEs and limiting the development of large-area PSCs [22]. Most recent research has focused on fabrication methods for large-area PSCs [10][22][23][24][25][26]. Apart from spin coating, other PSC fabrication methods include spray pyrolysis, dip coating [23][27][28], two-step interdiffusion [29][30], chemical vapor deposition, ink-jet printing, atomic layer deposition, and blade coating deposition [31][32][33][34]. These methods will be discussed in detail, with supportive diagrams provided where necessary.

Figure 2 from the NREL website shows the best solar cell efficiencies reported so far [35]. Certified PCEs as high as 25.5% were attained from single-junction PSCs with active areas of 0.0937 cm^2. However, the present average PCE for PSCs larger than 10 cm^2 (minimodules) is 18.04% (19.276 cm^2) [36], which falls below the PCE of a 79 cm^2 silicon PV cell, which is 26.7%. **Figure 2** shows nearly 50 articles published during the past years, including research on the PCEs of mesoporous and planar (usual and inverted) structural large-area PSC minimodules, of which the typical active area is from 10 to 100 cm^2; the five cases with sizes larger than 100 cm^2 are labeled.

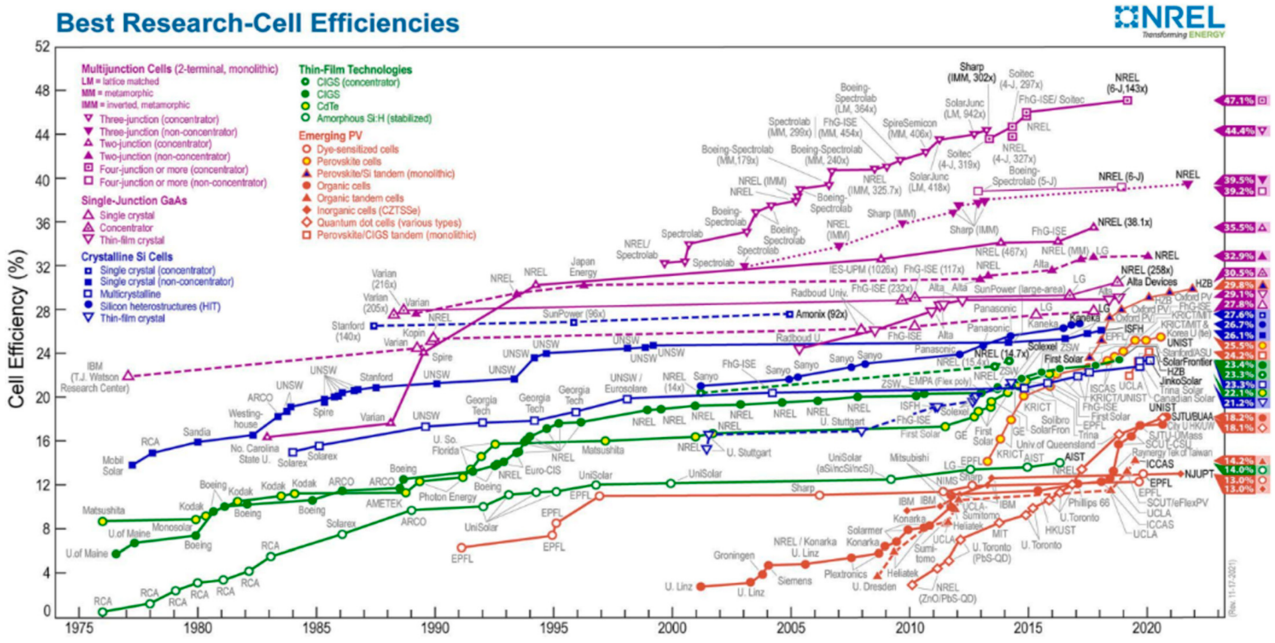

Figure 2. Best solar cell efficiencies, taken from the National Renewable Energy Laboratory (NREL) [35].

2. Large-Area PSC Preparation Methods and Fabrication Technologies

There are three critical factors for successful PSC commercialization: performance, cost, and stability. Improvements in device architecture and fabrication processes that have improved device performance have also resulted in PSC commercialization becoming an unstoppable trend. Commercialization of PSCs is now gradually being realized with the establishment of pilot production lines for perovskite photovoltaic devices possessing good performance and manufactured cost effectively using established techniques. However, device stability has continued to be an issue for researchers and industries.

Thin metal–organic perovskite films have traditionally been fabricated through solution-processed spin-coating, which permits fast iteration, optimization, and research development but is not a scalable technique for fabricating photovoltaic cells. The critical requirement for a scalable production method is low cost, which consists of capital expenditures for the necessary equipment as well as operational expenditures, including energy usage, material costs, the cost of post-treating production waste, and quality control [27][37][38]. Since the cost of contemporary PSC materials is negligible due to their ready availability, the costs of PSC manufacturing are dominated by capital expenditures and lowered by higher and faster throughputs [39]. Due to the different substrate materials, it is essential to distinguish between rigid and flexible PSCs when studying their synthesis methods. The large-area solar cell preparation methods shown in **Table 1** have been successfully used to manufacture flexible and rigid PSCs [16][40][41]. Perovskite thin-film fabrication methods are divided into solution processing and vapor deposition methods [7][40]. **Table 1** shows the different methods in each of these clusters. In contrast, **Figure 3** shows the graphic timeline on thin-film PSC fabrication methods for inorganic and hybrid halide perovskites developed by [42] shows that for the five years, most researchers have mainly focused on solution-based then vacuum base method.

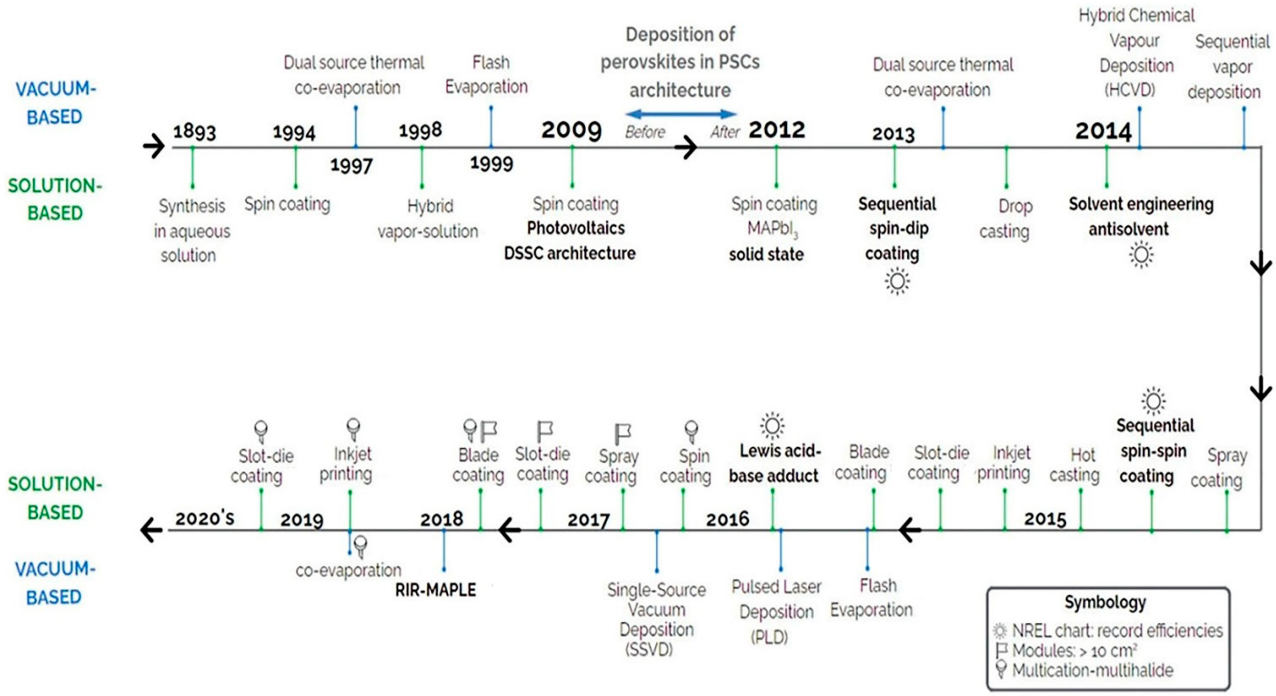

Figure 3. Timeline for application of vacuum deposition methods vs. solution processing methods in the fabrication of inorganic and mixed halide perovskites. The symbology legend defines fabrication methods used; reported National Renewable Energy Laboratory (NREL) record efficiencies, modules, and multi-cation/multi-halide compositions [42].

Table 1. Large-area perovskite thin-film fabrication methods used in the current work [15][17][23][40][41][43].

Solution Processing Method	Vapor Deposition Method
Spray coating	Vacuum thermal evaporation
Ink-jet printing	Co-evaporation
Spin coating	Sequential evaporation
Slot-die coating	Flash evaporation
Blade coating/Knife-over edge coating	Vapor assisted solution process
Vacuum flash-assisted solution process	Chemical vapor deposition

Some conclusions can be drawn from the two cluster methods in **Table 1** and related works of literature:

- In recent years, vacuum thermal evaporation has lost its position as the fabrication method of choice.
- Spray coating and blade coating have also seen a reduction in use by PSC researchers.
- PSC researchers have increasingly adopted ink-jet printing and slot-die coating.
- PSC researchers are working on overcoming the technological impediments to the synthesis and commercialization of large-area PSCs.
- Not all perovskite thin-film fabrication technologies have been used to create large-area solar cells despite some methods such as thermal evaporation having significant scalability potential.
- In recent publications, the slot-die coating has demonstrated the highest PCE for large-area PSCs, implying that it has a high potential for ushering in PSC commercialization.

Progress in the fabrication of large-area PSCs indicates that PSC commercialization is now a reality. As a matter of fact, Saule Technologies, a start-up from Poland, launched the world's first industrial production line of solar panels based on groundbreaking perovskite technology in May 2021. The company manufactures perovskite solar modules on thin, flexible

substrates, in a variety of different colors, using a novel, room-temperature ink-jet printing procedure invented by one of the company co-founders, Olga Malinkiewicz. Malinkiewicz developed this fabrication technique in 2013 while still a Ph.D. student at the University of Valencia in Spain and this work was published in Nature Photonics in 2013 [44].

2.1. Spin Coating

Spin coating is a batch method in which a liquid film is spread by centrifugal force onto a rotating substrate [45]. The method has been extensively used to manufacture small PSCs of about 0.1 cm^2 and large-area devices of 1 cm^2. This method is categorized into one-step and two-step processes. Perovskite devices fabricated through spin coating have reached PCEs of over 9.4% [46].

Spin coating has potential for the production of moderately large-area PSCs if evaporation of the solvent can be closely regulated [2][40], and this has been demonstrated by the authors of [47], who prepared a large-area perovskite film of 57 cm^2. The two-step sequential processing method provides better performance than the one-step method for perovskite deposition. In addition, film quality can be enhanced through controlled crystal growth and the post-annealing time [32][48].

2.2. Spray Coating Methods: Spray Printing, Spray Deposition, Spray Pyrolysis, and Ultrasonic Spray

Spray coating is a low-temperature and low-ink-concentration coating method that is suitable for large-area technology and it is a widely used deposition method in the industry [16]. It is an easily scalable method for fabricating large-area thin perovskite films. Perovskite film obtained through this method displays high uniformity over large areas.

Spray coating is accomplished through a series of four distinct activities: production of the ink droplets, placement of the droplets on the substrate, amalgamation of the droplets into a wet film, and film drying. Of all the scalable methods, spray coating is the most diverse. It presently encompasses two methods of deposition: one-step and two-step. One-step film deposition solutions comprise aprotic solvents [16][49][50][51]. Two-step methods use metal salts deposited by either spray coating or spin coating in an aprotic solvent lacking an acidic proton and hydroxyl and amine groups [40][52].

Spray coating is the fastest process by which a subjected fluid can be automatically driven to exhibit capillary waves and obtain a scalable substrate [21]. It is based on the atomization of a fluid and the depositing of the atomized fluid droplets onto a suitable surface. Atomization can be generated through various methods: high flow gas, ultrasonic stimulation, or cavitation of the ink itself [51][53]. The aforementioned atomization methods are generally scalable.

Ultrasonic spray coaters are the latest technology for efficiently preparing various functional thin films for photovoltaic cells [54][55]. Liquid thin-film coating technology has been developed for different applications.

Organic salts are deposited on the substrate by spray coating or immersion in an alcohol solution, using isopropanol as the solvent [56][57][58][59]. The results vary depending on the method of perovskite solution deposition employed. The single-step deposition method has been used in compositions encompassing MAI, lead iodide, and iodide chloride varieties [56][60]. The solvents used were DMF, DMSO, gamma-butyrolactone (GBL), DMF-DMSO, and GBL-DMSO; some studies used processing additives such as hydrogen iodide (HI) [60]. The highest reported PCE for perovskite films made through this method was 18% for small-area samples and 15.5% for the maximum device area of 40 cm^2 [61].

Robert et al. reported the device area with the highest efficiency and good morphology without using an ultrasonic spray coater [52]. They used single-cation (MAI) mixed halide for perovskite preparation by spray coating on a preheated substrate, and this showed excellent crystallization morphology [49][51]. Ultrasonic atomization plays a crucial role in nucleation, metal polyhalide complex formation, solution optimization processes, and temperature control.

Kim et al. developed devices using the antisolvent spray coating method, which allows high-quality perovskite film to be deposited over a large area. An FTO/glass/bl-TiO_2/m-TiO_2/perovskite/spiro-OMeTAD/gold 16 cm^2 device on the cellular level, as opposed to the module level, was created via the modified solution process in combination with a metal lattice. This cell device was found to be 12.1% efficient and overcame low PCE and poor film quality challenges associated with large-area PSCs [22].

Tait et al. used concurrently pumped ultrasonic spray coating for precise and fast optimization of the precursor ratios of $PbCl_2$, $Pb(CH_3CO_2)_2{\cdot}3H_2O$, $PbBr_2$, MABr, and MAI to attain pinhole-free perovskite films with high crystallinity, and they achieved a PCE of 11.7% for 3.8 cm^2 modules [16][50].

Ye et al. manufactured high-efficiency large-area PSCs using NiO-based HTLs synthesized through a spray pyrolysis method. PSCs with active areas of 1 cm^2 exhibited notable mean PCEs of 17.6% [62], 18.21% [63], and 19.19% [64]. A

larger PSC with an active area of 5 cm^2 attained a mean PCE of 15.5% [65]. The PSC based on the mesoscopic TiO_2/Al_2O_3/NiO/carbon framework showed a PCE of up to 15.03% [66]. Using a recent facile spray deposition method for CuI film, PSCs exhibited a mean PCE of 17.6% and excellent device stability [67]. The method frequently used in large-area C-TiO_2 for electron transport material fabrication is spray pyrolysis deposition [34][67][68][69][70][71][72]. Compared to the traditional spin coating method, the pyrolysis spray deposition method produces a denser TiO_2 film, lessening material loss and deposition time, which results in desirable low-cost production.

Nanomaterial spray coating has been widely investigated as a means for developing semi-transparent devices due to its simple process. For example, using transparent electrodes of spray-coated silver nanowires, carbon nanotubes, and the respective composites, small 0.25 cm^2 entirely solution-processed, semi-transparent PSCs with more than 10% PCEs were successfully fabricated [73][74][75][76][77].

2.3. Slot-Die Coating Method

Slot-die coating is a process in which ink is metered through a microfluidic metal die machine. The die is machine structured with a thin channel to spread ink over a moving substrate surface [45].

2.4. Blade-Coating Method

Blade coating is a method in which a blade moves across a surface or vice-versa in the case of roll-to-roll coating [45][78]; it is also known as doctor-blading and knife-over-edge coating. The blade spreads pre-dispensed ink and forms it into a thin liquid film. The film is then dried, creating a solid thin film. This is the most used synthesis technique for fabricating large-area perovskite films. It has been used in several PSC studies to synthesize high-performance cells with areas of over 10 cm^2. Various studies have demonstrated that the perovskite film quality can be enhanced by controlling the processing temperature [79][80]. Recently, additives have been utilized to realize dense perovskite films with smaller pinholes and homogeneous crystal morphology [81][82]. Blade coating has been commonly used as a single-step deposition method for perovskite films [33][34][78][83][84][85][86][87] and recently for producing perovskite PVs with a 20% [83][84][88] scalable solution method.

Razza et al. used this method to fabricate a PSC module with an active area of 10.1 cm^2 and recorded an average PCE of 10.4% [34], while previously, these authors reported a PCE of 4.3% for a cell area of 100 cm^2 [34]. Gao et al. reported a method for fabricating ultra-long nanowire arrays and highly oriented CH_3-NH_3PbI_3 thin films in ambient environments. This method integrated large-scale roll-to-roll micro gravure printing and doctor blading to fabricate perovskite nanowires of 15 mm in length [89].

2.5. Ink-Jet Printing Method

This is a non-contact printing method with direct control of ink deposition, which greatly reduces material utilization and waste. Quintilla et al. reported the fabrication and optimization of multipass inkjet-printed PSCs [90]. The perovskite film's thickness and grain size were carefully controlled during multipass ink-jet printing with $MAPbI_3$ ink, producing PSCs with a high average PCE of 11.3% [90].

Ink-jet printing is a method through which a microfluidic cavity is subjected to pressure change, thereby causing the solution to jet out of a microfluidic nozzle. This pressure change can be created through various methods, including thermal and structural sources acting on the microfluidic nozzle. Most ink-jet printing methods demonstrate piezoelectricity of the ink-jet printhead based on a micro-electro-mechanical system, which provides controllable microfluidic jetting through a silicon-etched nozzle. Ink-jet printing, such as ink-jet printers, uses numerous jetting nozzles in a single mobile print head to control the planar thin film thickness and improve the reliability and speed [91].

2.6. Vacuum Flash-Assisted Solution Method

The vacuum flash-assisted solution (VAS) method allows fast and well-controlled removal of the solvent. In so doing, it promotes rapid crystallization of the perovskite precursor phase [92].

2.7. Chemical Vapor Deposition Method

Chemical vapor deposition (CVD) is an established, low-cost, and highly efficient technology for fabricating various semiconductor materials from gases. Compared to the PSC device fabrication process using the spin coating method, CVD methods produce significantly higher device performance. The CVD variants include dual-source evaporation [93], vapor–solid reaction [94], and the vapor-assisted method, [14]. Liu et al. fabricated high-quality and uniform perovskite films using the dual-source co-evaporation method [93]. This method is reliant on high temperatures and high vacuum

conditions. Alternatively, the vapor–solid reaction method can be used as a substitute, which deposits the perovskite film at a low temperature [94]. Chen et al. used this method on a 64 cm^2 PSC device and obtained a mean PCE of 6.0% over an active area of 1.5 cm^2 [94].

2.8. Sequential Evaporation Method

This method involves the separate vapor deposition of multiple film layers on top of each other and the subsequent conversion of these multiple film layers through diffusion and recrystallization. First, the metal halide layer is deposited on top of the conductive glass and then on the organic halides. The sequential deposition demonstration of MAPbI perovskite films showed a significantly lower small-scale PCE of 5.4% for a device without a hole-transporting layer [95]. However, this method might not be ideal for optimum commercial scaling as the throughput and alternating evaporation might slow material utilization. The highest efficiency achieved for sequentially evaporated PSCs was 17.6% for small-area devices; this was accomplished by optimizing the system's pressures through the evaporation steps, which also had a binding effect on the morphology [96].

2.9. Co-Evaporation Method

This method is the most applicable vacuum-based process for several applications. The perovskite films are prepared inside a high-vacuum chamber with a pressure of 10^{-5}–10^{-6} mbar, where the precursor solutions are loaded in separate crucibles and heated to their corresponding sublimation temperatures [97]. Co-vapor-deposited PSC films are smooth and homogeneous, with modules achieving high PCEs of 16.5% [98]. Additionally, the method enables the preparation of multilayer films and is completely compatible with conventional semiconductor manufacturing methods.

2.10. Flash Evaporation Method

In this process, the perovskite materials are positioned on a metallic heater and transferred to a vacuum. A large high-current voltage is transmitted through the metal heater, which activates all the perovskite substance, causing it to swiftly vaporize and condense onto a substrate to form a thin perovskite film. Longo et al. established that the flash evaporation method could be applied for the deposition perovskite materials [98].

Two-dimensional (2D) and three-dimensional (3D) layered metal halide perovskites doped with aliphatic or aromatic ammonium cations have been synthesized through this method. The hybrid film is synthesized at temperatures that are sufficiently high for the inorganic material to volatilize without deteriorating the organic part [40][98][99]. Homogeneous and smooth polycrystalline $MAPbI_3$ thin films of the required thickness can be achieved by carefully adjusting the process variables. The final layer's thickness and homogeneity are attained if the metal heater is coated with the deposited material. Longo et al. obtained a PCE of 12.2% for a PSC fabricated through this technique [98].

2.11. Vacuum Thermal Evaporation Method

With this method, materials are sublimated by heating them under high vacuum conditions (pressures ≤ 10^{-6} Pa) and allowing the resulting vapor to condense onto a cooler substrate [40]. The evaporated particles are extended under high vacuum conditions. The sublimated particles move away from the heated source in a deposition cone to reach the substrate. The film's deposition uniformity depends on the distance from the evaporation source to the substrate. The reduced material production resulting from parasitic condensation on the vacuum chamber walls is a trade-off [40]. Large-scale manufacturing processes use linear deposition sources with a substrate that moves orthogonally through the elongated evaporation cone.

Cimaroli et al. used the vacuum thermal evaporation method to produce perovskite films for the comparison of low-temperature processed SnO_2 at 185 °C with high-temperature processed SnO_2 at 500 °C [100].

2.12. Multi-Flow Air Knife Method

Gao et al. fabricated highly efficient PSCs composed of a perovskite film dried using the innovative multi-flow air knife (MAK) method in ambient conditions. Through this method, these authors produced large-grain, homogeneous, and pinhole-free perovskite films of 4.98 nm thickness. The same authors subsequently achieved a PCE of 11.70% for large-area PSCs with an active area of 1 cm^2 and obtained a high PCE of 17.71% with an active area of 0.1 cm^2 [101], suggesting that the MAK method is promising. However, this high PCE was achieved by optimizing the airflow rate to 300 L min^{-1} and the distance between the air knife and the substrate surface to 1 mm.

References

1. Kour, R.; Arya, S.; Verma, S.; Gupta, J.; Bandhoria, P.; Bharti, V.; Datt, R.; Gupta, V. Potential Substitutes for Replacement of Lead in Perovskite Solar Cells: A Review. Glob. Chall. 2019, 3, 1900050.
2. Rajagopal, A.; Yao, K.; Jen, A.K.Y. Toward Perovskite Solar Cell Commercialization: A Perspective and Research Roadmap Based on Interfacial Engineering. Adv. Mater. 2018, 30, 1800455.
3. Enriquez, C.; Hodges, D.; De La Rosa, A.; Valerio Frias, L.; Ramirez, Y.; Rodriguez, V.; Rivera, D.; Telle, A. Perovskite Solar Cells. In Proceedings of the 2019 IEEE 46th Photovoltaic Specialists Conference (PVSC), Chicago, IL, USA, 16–21 June 2019.
4. Hamukwaya, S.L.; Zhao, Z.; Wang, N.; Liu, H.; Umar, A.; Zhang, J.; Wu, T.; Guo, Z. Enhanced Photocatalytic Activity of B, N-Codoped TiO2 by a New Molten Nitrate Process. J. Nanosci. Nanotechnol. 2018, 19, 839–849.
5. Lewis, N.S.; Nocera, D.G. Powering the planet: Chemical challenges in solar energy utilization. Proc. Natl. Acad. Sci. USA 2006, 103, 15729–15735.
6. Wang, R.; Mujahid, M.; Duan, Y.; Wang, Z.K.; Xue, J.; Yang, Y. A Review of Perovskites Solar Cell Stability. Adv. Funct. Mater. 2019, 29, 1808843.
7. Li, D.; Shi, J.; Xu, Y.; Luo, Y.; Wu, H.; Meng, Q. Inorganic-organic halide perovskites for new photovoltaic technology. Natl. Sci. Rev. 2018, 5, 559–576.
8. Niu, G.; Guo, X.; Wang, L. Review of recent progress in chemical stability of perovskite solar cells. J. Mater. Chem. A 2015, 3, 8970–8980.
9. Parisi, M.L.; Maranghi, S.; Basosi, R. The evolution of the dye sensitized solar cells from Grätzel prototype to up-scaled solar applications: A life cycle assessment approach. Renew. Sustain. Energy Rev. 2014, 39, 124–138.
10. Uddin, A.; Upama, M.B.; Yi, H.; Duan, L. Encapsulation of organic and perovskite solar cells: A review. Coatings 2019, 9, 65.
11. Tang, H.; He, S.; Peng, C. A Short Progress Report on High-Efficiency Perovskite Solar Cells. Nanoscale Res. Lett. 2017, 12, 410.
12. Wang, F.; Cao, Y.; Chen, C.; Chen, Q.; Wu, X.; Li, X.; Qin, T.; Huang, W. Materials toward the Upscaling of Perovskite Solar Cells: Progress, Challenges, and Strategies. Adv. Funct. Mater. 2018, 28, 1803753.
13. Pitchaiya, S.; Natarajan, M.; Santhanam, A.; Asokan, V.; Yuvapragasam, A.; Madurai Ramakrishnan, V.; Palanisamy, S.E.; Sundaram, S.; Velauthapillai, D. A review on the classification of organic/inorganic/carbonaceous hole transporting materials for perovskite solar cell application. Arab. J. Chem. 2020, 13, 2526–2557.
14. Assadi, M.K.; Bakhoda, S.; Saidur, R.; Hanaei, H. Recent progress in perovskite solar cells. Renew. Sustain. Energy Rev. 2018, 81, 2812–2822.
15. Chen, Y.; Zhang, L.; Zhang, Y.; Gao, H.; Yan, H. Large-area perovskite solar cells-a review of recent progress and issues. RSC Adv. 2018, 8, 10489–10508.
16. Zhao, Y.; Ma, F.; Gao, F.; Yin, Z.; Zhang, X.-W.; You, J. Research Progresses in Large-Area Perovskite Solar Cells. Photonics Res. 2020, 8, A1–A15.
17. Li, X.; Bi, D.; Yi, C.; Décoppet, J.D.; Luo, J.; Zakeeruddin, S.M.; Hagfeldt, A.; Grätzel, M. A vacuum flash-assisted solution process for high-efficiency large-area perovskite solar cells. Science 2016, 353, 58–62.
18. Lee, J.W.; Lee, D.K.; Jeong, D.N.; Park, N.G. Control of Crystal Growth toward Scalable Fabrication of Perovskite Solar Cells. Adv. Funct. Mater. 2019, 29, 1807047.
19. Kim, D.H.; Whitaker, J.B.; Li, Z.; van Hest, M.F.A.M.; Zhu, K. Outlook and Challenges of Perovskite Solar Cells toward Terawatt-Scale Photovoltaic Module Technology. Joule 2018, 2, 1437–1451.
20. Park, N.G. Research Direction toward Scalable, Stable, and High Efficiency Perovskite Solar Cells. Adv. Energy Mater. 2020, 10, 1903106.
21. Dai, X.; Xu, K.; Wei, F. Recent progress in perovskite solar cells: The perovskite layer. Beilstein J. Nanotechnol. 2020, 11, 51–60.
22. Kim, J.; Yun, J.S.; Cho, Y.; Lee, D.S.; Wilkinson, B.; Soufiani, A.M.; Deng, X.; Zheng, J.; Shi, A.; Lim, S.; et al. Overcoming the Challenges of Large-Area High-Efficiency Perovskite Solar Cells. ACS Energy Lett. 2017, 2, 1978–1984.
23. Park, N.G.; Zhu, K. Scalable fabrication and coating methods for perovskite solar cells and solar modules. Nat. Rev. Mater. 2020, 5, 333–350.

24. Gao, F.; Zhao, Y.; Zhang, X.; You, J. Recent Progresses on Defect Passivation toward Efficient Perovskite Solar Cells. Adv. Energy Mater. 2020, 10, 1902650.

25. Dai, T.; Cao, Q.; Yang, L.; Aldamasy, M.H.; Li, M.; Liang, Q.; Lu, H.; Dong, Y.; Yang, Y. Strategies for High-Performance Large-Area Perovskite Solar Cells toward Commercialization. Crystals 2021, 11, 295.

26. Niu, T.; Zhu, W.; Zhang, Y.; Xue, Q.; Jiao, X.; Wang, Z.; Xie, Y.M.; Li, P.; Chen, R.; Huang, F.; et al. D-A-π-A-D-type Dopant-free Hole Transport Material for Low-Cost, Efficient, and Stable Perovskite Solar Cells. Joule 2021, 5, 249–269.

27. Li, Z.; Klein, T.R.; Kim, D.H.; Yang, M.; Berry, J.J.; Van Hest, M.F.A.M.; Zhu, K. Scalable fabrication of perovskite solar cells. Nat. Rev. Mater. 2018, 3, 18017.

28. Bae, I.G.; Park, B. All-self-metered solution-coating process in ambient air for the fabrication of efficient, large-area, and semitransparent perovskite solar cells. Sustain. Energy Fuels 2020, 4, 3115–3128.

29. Burschka, J.; Pellet, N.; Moon, S.J.; Humphry-Baker, R.; Gao, P.; Nazeeruddin, M.K.; Grätze, M. Sequential deposition as a route to high-performance perovskite-sensitized solar cells. Nature 2013, 499, 316–319.

30. Xiao, Z.; Bi, C.; Shao, Y.; Dong, Q.; Wang, Q.; Yuan, Y.; Wang, C.; Gao, Y.; Huang, J. Efficient, high yield perovskite photovoltaic devices grown by interdiffusion of solution-processed precursor stacking layers. Energy Environ. Sci. 2014, 7, 2619–2623.

31. Liu, X.; Cao, L.; Guo, Z.; Li, Y.; Gao, W.; Zhou, L. A review of perovskite photovoltaic materials' synthesis and applications via chemical vapor deposition method. Materials 2019, 12, 3304.

32. Shalan, A.E. Challenges and approaches towards upscaling the assembly of hybrid perovskite solar cells. Mater. Adv. 2020, 1, 292–309.

33. Hwang, K.; Jung, Y.S.; Heo, Y.J.; Scholes, F.H.; Watkins, S.E.; Subbiah, J.; Jones, D.J.; Kim, D.Y.; Vak, D. Toward large scale roll-to-roll production of fully printed perovskite solar cells. Adv. Mater. 2015, 27, 1241–1247.

34. Razza, S.; Di Giacomo, F.; Matteocci, F.; Cinà, L.; Palma, A.L.; Casaluci, S.; Cameron, P.; Epifanio, A.D.; Licoccia, S.; Reale, A.; et al. Perovskite solar cells and large area modules (100 cm2) based on an air flow-assisted PbI2 blade coating deposition process. J. Power Sources 2015, 277, 286–291.

35. NREL. Best-Research-Cell-Efficiencies-Rev211117. Available online: https://www.nrel.gov/pv/assets/pdfs/best-research-cell-efficiencies-rev211117.pdf (accessed on 22 January 2022).

36. Zhihui Photovolt. The Efficiency of Perovskite Components Exceeds 18%, and There Is Huge Room for Imagination in the Future! 2020. Available online: Http://solar.in-en.com/html/solar-2352538.shtml (accessed on 18 January 2022).

37. Jean, J.; Xiao, J.; Nick, R.; Moody, N.; Nasilowski, M.; Bawendi, M.; Bulović, V. Synthesis cost dictates the commercial viability of lead sulfide and perovskite quantum dot photovoltaics. Energy Environ. Sci. 2018, 11, 2295–2305.

38. Song, Z.; McElvany, C.L.; Phillips, A.B.; Celik, I.; Krantz, P.W.; Watthage, S.C.; Liyanage, G.K.; Apul, D.; Heben, M.J. A technoeconomic analysis of perovskite solar module manufacturing with low-cost materials and techniques. Energy Environ. Sci. 2017, 10, 1297–1305.

39. Zhang, Q.; Hao, F.; Li, J.; Zhou, Y.; Wei, Y.; Lin, H. Perovskite solar cells: Must lead be replaced-and can it be done? Sci. Technol. Adv. Mater. 2018, 19, 425–442.

40. Swartwout, R.; Hoerantner, M.T.; Bulović, V. Scalable Deposition Methods for Large-Area Production of Perovskite Thin Films. Energy Environ. Mater. 2019, 2, 119–145.

41. Yang, Z.; Zhang, S.; Li, L.; Chen, W. Research progress on large-area perovskite thin films and solar modules. J. Mater. 2017, 3, 231–244.

42. Soto-Montero, T.; Soltanpoor, W.; Morales-Masis, M. Pressing challenges of halide perovskite thin film growth. APL Mater. 2020, 8, 110903.

43. Borchert, J.; Milot, R.L.; Patel, J.B.; Davies, C.L.; Wright, A.D.; Martínez Maestro, L.; Snaith, H.J.; Herz, L.M.; Johnston, M.B. Large-Area, Highly Uniform Evaporated Formamidinium Lead Triiodide Thin Films for Solar Cells. ACS Energy Lett. 2017, 2, 2799–2804.

44. Malinkiewicz, O.; Yella, A.; Lee, Y.H.; Espallargas, G.M.; Graetzel, M.; Nazeeruddin, M.K.; Bolink, H.J. Perovskite solar cells employing organic charge-transport layers. Nat. Photon. 2014, 8, 128–132.

45. Larson, R.G.; Rehg, T.J. Spin Coating. In Liquid Film Coating; Chapman & Hall: Glasgow, UK, 1997.

46. Tzounis, L.; Stergiopoulos, T.; Zachariadis, A.; Gravalidis, C.; Laskarakis, A.; Logothetidis, S. Perovskite solar cells from small scale spin coating process towards roll-to-roll printing: Optical and Morphological studies. Mater. Today Proc. 2017, 4, 5082–5089.

47. Kim, M.K.; Lee, H.S.; Pae, S.R.; Kim, D.J.; Lee, J.Y.; Gereige, I.; Park, S.; Shin, B. Effects of temperature and coating speed on the morphology of solution-sheared halide perovskite thin-films. J. Mater. Chem. A 2018, 6, 24911–24919.

48. Han, G.S.; Kim, J.; Bae, S.; Han, S.; Kim, Y.J.; Gong, O.Y.; Lee, P.; Ko, M.J.; Jung, H.S. Spin-Coating Process for 10 cm × 10 cm Perovskite Solar Modules Enabled by Self-Assembly of SnO2 Nanocolloids. ACS Energy Lett. 2019, 4, 1845–1851.

49. Barrows, A.T.; Pearson, A.J.; Kwak, C.K.; Dunbar, A.D.F.; Buckley, A.R.; Lidzey, D.G. Efficient planar heterojunction mixed-halide perovskite solar cells deposited via spray-deposition. Energy Environ. Sci. 2014, 7, 2944–2950.

50. Tait, J.G.; Manghooli, S.; Qiu, W.; Rakocevic, L.; Kootstra, L.; Jaysankar, M.; Masse De La Huerta, C.A.; Paetzold, U.W.; Gehlhaar, R.; Cheyns, D.; et al. Rapid composition screening for perovskite photovoltaics via concurrently pumped ultrasonic spray coating. J. Mater. Chem. A 2016, 4, 3792–3797.

51. Das, S.; Yang, B.; Gu, G.; Joshi, P.C.; Ivanov, I.N.; Rouleau, C.M.; Aytug, T.; Geohegan, D.B.; Xiao, K. High-Performance Flexible Perovskite Solar Cells by Using a Combination of Ultrasonic Spray-Coating and Low Thermal Budget Photonic Curing. ACS Photonics 2015, 2, 680–686.

52. Yao, J.; Yang, L.; Cai, F.; Yan, Y.; Gurney, R.S.; Liu, D.; Wang, T. The impacts of PbI2 purity on the morphology and device performance of one-step spray-coated planar heterojunction perovskite solar cells. Sustain. Energy Fuels 2018, 2, 436–443.

53. Kim, H.S.; Im, S.H.; Park, N.G. Organolead halide perovskite: New horizons in solar cell research. J. Phys. Chem. C 2014, 118, 5615–5625.

54. Siansonic. Ultrasonic and Piezoelectric Technologies. 2020. Available online: Https://www.Siansonic.Com/Products (accessed on 22 January 2022).

55. Sono-Tek. Ultrasonic System. Available online: http://www.siansonic.com/ (accessed on 22 January 2022).

56. Gamliel, S.; Dymshits, A.; Aharon, S.; Terkieltaub, E.; Etgar, L. Micrometer Sized Perovskite Crystals in Planar Hole Conductor Free Solar Cells. J. Phys. Chem. C 2015, 119, 19722–19728.

57. Huang, H.; Shi, J.; Zhu, L.; Li, D.; Luo, Y.; Meng, Q. Two-step ultrasonic spray deposition of CH3NH3PbI3 for efficient and large-area perovskite solar cell. Nano Energy 2016, 27, 352–358.

58. Remeika, M.; Raga, S.R.; Zhang, S.; Qi, Y. Transferrable optimization of spray-coated PbI2 films for perovskite solar cell fabrication. J. Mater. Chem. A 2017, 5, 5709–5718.

59. Chai, G.; Luo, S.; Zhou, H.; Daoud, W.A. CH3NH3PbI3−xBrx perovskite solar cells via spray assisted two-step deposition: Impact of bromide on stability and cell performance. Mater. Des. 2017, 125, 222–229.

60. Bishop, J.E.; Mohamad, D.K.; Wong-Stringer, M.; Smith, A.; Lidzey, D.G. Spray-cast multilayer perovskite solar cells with an active-area of 1.5 cm2. Sci. Rep. 2017, 7, 7962.

61. Heo, J.H.; Lee, M.H.; Jang, M.H.; Im, S.H. Highly efficient CH3NH3PbI3-xClx mixed halide perovskite solar cells prepared by re-dissolution and crystal grain growth via spray coating. J. Mater. Chem. A 2016, 4, 17636–17642.

62. Ye, F.; Chen, H.; Xie, F.; Tang, W.; Yin, M.; He, J.; Bi, E.; Wang, Y.; Yang, X.; Han, L. Soft-cover deposition of scaling-up uniform perovskite thin films for high cost-performance solar cells. Energy Environ. Sci. 2016, 9, 2295–2301.

63. Wu, Y.; Yang, X.; Chen, W.; Yue, Y.; Cai, M.; Xie, F.; Bi, E.; Islam, A.; Han, L. Perovskite solar cells with 18.21% efficiency and area over 1 cm2 fabricated by heterojunction engineering. Nat. Energy 2016, 1, 16148.

64. Wu, Y.; Xie, F.; Chen, H.; Yang, X.; Su, H.; Cai, M.; Zhou, Z.; Noda, T.; Han, L. Thermally Stable MAPbI3 Perovskite Solar Cells with Efficiency of 19.19% and Area over 1 cm2 achieved by Additive Engineering. Adv. Mater. 2017, 29, 1701073.

65. Di Giacomo, F.; Fakharuddin, A.; Jose, R.; Brown, T.M. Progress, challenges and perspectives in flexible perovskite solar cells. Energy Environ. Sci. 2016, 9, 3007–3035.

66. Cao, K.; Zuo, Z.; Cui, J.; Shen, Y.; Moehl, T.; Zakeeruddin, S.M.; Grätzel, M.; Wang, M. Efficient screen printed perovskite solar cells based on mesoscopic TiO2/Al2O3/NiO/carbon architecture. Nano Energy 2015, 17, 171–179.

67. Li, X.; Yang, J.; Jiang, Q.; Chu, W.; Zhang, D.; Zhou, Z.; Xin, J. Synergistic Effect to High-Performance Perovskite Solar Cells with Reduced Hysteresis and Improved Stability by the Introduction of Na-Treated TiO2 and Spraying-Deposited CuI as Transport Layers. ACS Appl. Mater. Interfaces 2017, 9, 41354–41362.

68. Yang, W.S.; Park, B.-W.W.; Jung, E.H.; Jeon, N.J.; Kim, Y.C.; Lee, D.U.; Shin, S.S.; Seo, J.; Kim, E.K.; Noh, J.H.; et al. Iodide management in formamidinium-lead-halide-based perovskite layers for efficient solar cells. Science 2017, 356, 1376–1379.

69. Chen, H.; Ye, F.; Tang, W.; He, J.; Yin, M.; Wang, Y.; Xie, F.; Bi, E.; Yang, X.; Grätzel, M.; et al. A solvent-and vacuum-free route to large-area perovskite films for efficient solar modules. Nature 2017, 550, 92–95.

70. Lu, J.; Jiang, L.; Li, W.; Li, F.; Pai, N.K.; Scully, A.D.; Tsai, C.M.; Bach, U.; Simonov, A.N.; Cheng, Y.B.; et al. Diammonium and Monoammonium Mixed-Organic-Cation Perovskites for High Performance Solar Cells with Improved Stability. Adv. Energy Mater. 2017, 7, 1700444.
71. Jiang, Y.; Leyden, M.R.; Qiu, L.; Wang, S.; Ono, L.K.; Wu, Z.; Juarez-Perez, E.J.; Qi, Y. Combination of Hybrid CVD and Cation Exchange for Upscaling Cs-Substituted Mixed Cation Perovskite Solar Cells with High Efficiency and Stability. Adv. Funct. Mater. 2018, 28, 1703835.
72. Matteocci, F.; Cinà, L.; Di Giacomo, F.; Razza, S.; Palma, A.L.; Guidobaldi, A.; D'Epifanio, A.; Licoccia, S.; Brown, T.M.; Reale, A.; et al. High efficiency photovoltaic module based on mesoscopic organometal halide perovskite. Prog. Photovolt. Res. Appl. 2016, 24, 436–445.
73. Kim, A.; Lee, H.; Kwon, H.C.; Jung, H.S.; Park, N.G.; Jeong, S.; Moon, J. Fully solution-processed transparent electrodes based on silver nanowire composites for perovskite solar cells. Nanoscale 2016, 8, 6308–6316.
74. Khoa, N.H.; Tanaka, Y.; Goh, W.P.; Jiang, C. A solution processed Ag-nanowires/C60 composite top electrode for efficient and translucent perovskite solar cells. Sol. Energy 2020, 196, 582–588.
75. Han, K.; Xie, M.; Zhang, L.; Yan, L.; Wei, J.; Ji, G.; Luo, Q.; Lin, J.; Hao, Y.; Ma, C.Q. Fully solution processed semi-transparent perovskite solar cells with spray-coated silver nanowires/ZnO composite top electrode. Sol. Energy Mater. Sol. Cells 2018, 185, 399–405.
76. Dou, Y.; Liu, Z.; Wu, Z.; Liu, Y.; Li, J.; Leng, C.; Fang, D.; Liang, G.; Xiao, J.; Li, W.; et al. Self-augmented ion blocking of sandwiched 2D/1D/2D electrode for solution processed high efficiency semitransparent perovskite solar cell. Nano Energy 2020, 71, 104567.
77. Habibi, M.; Rahimzadeh, A.; Bennouna, I.; Eslamian, M. Defect-Free Large-Area (25 cm2) Light Absorbing Perovskite Thin Films Made by Spray Coating. Coatings 2017, 7, 42.
78. Deng, Y.; Zheng, X.; Bai, Y.; Wang, Q.; Zhao, J.; Huang, J. Surfactant-controlled ink drying enables high-speed deposition of perovskite films for efficient photovoltaic modules. Nat. Energy 2018, 3, 560–566.
79. Deng, Y.; Wang, Q.; Yuan, Y.; Huang, J. Vividly colorful hybrid perovskite solar cells by doctor-blade coating with perovskite photonic nanostructures. Mater. Horiz. 2015, 2, 578–583.
80. Deng, Y.; Peng, E.; Shao, Y.; Xiao, Z.; Dong, Q.; Huang, J. Scalable fabrication of efficient organolead trihalide perovskite solar cells with doctor-bladed active layers. Energy Environ. Sci. 2015, 8, 1544–1550.
81. Li, C.; Yin, J.; Chen, R.; Lv, X.; Feng, X.; Wu, Y.; Cao, J. Monoammonium Porphyrin for Blade-Coating Stable Large-Area Perovskite Solar Cells with >18% Efficiency. J. Am. Chem. Soc. 2019, 141, 6345–6351.
82. Wu, W.Q.; Yang, Z.; Rudd, P.N.; Shao, Y.; Dai, X.; Wei, H.; Zhao, J.; Fang, Y.; Wang, Q.; Liu, Y.; et al. Bilateral alkylamine for suppressing charge recombination and improving stability in blade-coated perovskite solar cells. Sci. Adv. 2019, 5, 2001906.
83. Lin, Y.; Ye, X.; Wu, Z.; Zhang, C.; Zhang, Y.; Su, H.; Yin, J.; Li, J. Manipulation of the crystallization of perovskite films induced by a rotating magnetic field during blade coating in air. J. Mater. Chem. A 2018, 6, 3986–3995.
84. Wu, W.Q.; Wang, Q.; Fang, Y.; Shao, Y.; Tang, S.; Deng, Y.; Lu, H.; Liu, Y.; Li, T.; Yang, Z.; et al. Molecular doping enabled scalable blading of efficient hole-transport-layer-free perovskite solar cells. Nat. Commun. 2018, 9, 1625.
85. Kong, W.; Wang, G.; Zheng, J.; Hu, H.; Chen, H.; Li, Y.; Hu, M.; Zhou, X.; Liu, C.; Chandrashekar, B.N.; et al. Fabricating High-Efficient Blade-Coated Perovskite Solar Cells under Ambient Condition Using Lead Acetate Trihydrate. Sol. RRL 2018, 2, 1700214.
86. Zhong, Y.; Munir, R.; Li, J.; Tang, M.-C.; Niazi, M.R.; Smilgies, D.-M.; Zhao, K.; Amassian, A. Blade-Coated Hybrid Perovskite Solar Cells with Efficiency > 17%: An In Situ Investigation. ACS Energy Lett. 2018, 3, 1078–1085.
87. Yang, Z.; Chueh, C.C.; Zuo, F.; Kim, J.H.; Liang, P.W.; Jen, A.K.Y. High-Performance Fully Printable Perovskite Solar Cells via Blade-Coating Technique under the Ambient Condition. Adv. Energy Mater. 2015, 5, 1500328.
88. Li, J.; Munir, R.; Fan, Y.; Niu, T.; Liu, Y.; Zhong, Y.; Yang, Z.; Tian, Y.; Liu, B.; Sun, J.; et al. Phase Transition Control for High-Performance Blade-Coated Perovskite Solar Cells. Joule 2018, 2, 1313–1330.
89. Hu, Q.; Wu, H.; Sun, J.; Yan, D.; Gao, Y.; Yang, J. Large-area perovskite nanowire arrays fabricated by large-scale roll-to-roll micro-gravure printing and doctor blading. Nanoscale 2016, 8, 5350–5357.
90. Mathies, F.; Abzieher, T.; Hochstuhl, A.; Glaser, K.; Colsmann, A.; Paetzold, U.W.; Hernandez-Sosa, G.; Lemmer, U.; Quintilla, A. Multipass inkjet printed planar methylammonium lead iodide perovskite solar cells. J. Mater. Chem. A 2016, 4, 19207–19213.
91. Karunakaran, S.K.; Arumugam, G.M.; Yang, W.; Ge, S.; Khan, S.N.; Lin, X.; Yang, G. Recent progress in inkjet-printed solar cells. J. Mater. Chem. A 2019, 7, 13873–13902.

92. Lee, J.W.; Kim, H.S.; Park, N.G. Lewis Acid-Base Adduct Approach for High-Efficiency Perovskite Solar Cells. Acc. Chem. Res. 2016, 49, 311–319.
93. Liu, M.; Johnston, M.B.; Snaith, H.J. Efficient planar heterojunction perovskite solar cells by vapor deposition. Nature 2013, 501, 395–398.
94. Chen, X.; Cao, H.; Yu, H.; Zhu, H.; Zhou, H.; Yang, L.; Yin, S. Large-area, high-quality organic-inorganic hybrid perovskite thin films: Via a controlled vapor-solid reaction. J. Mater. Chem. A 2016, 4, 9124–9132.
95. Hu, H.; Wang, D.; Zhou, Y.; Zhang, J.; Lv, S.; Pang, S.; Chen, X.; Liu, Z.; Padture, N.P.; Cui, G. Vapour-based processing of hole-conductor-free CH3NH3PbI3 perovskite/C60 fullerene planar solar cells. RSC Adv. 2014, 4, 28964–28967.
96. Hsiao, S.Y.; Lin, H.L.; Lee, W.H.; Tsai, W.L.; Chiang, K.M.; Liao, W.Y.; Ren-Wu, C.Z.; Chen, C.Y.; Lin, H.W. Efficient All-Vacuum Deposited Perovskite Solar Cells by Controlling Reagent Partial Pressure in High Vacuum. Adv. Mater. 2016, 28, 7013–7019.
97. Ávila, J.; Momblona, C.; Boix, P.P.; Sessolo, M.; Bolink, H.J. Vapor-Deposited Perovskites: The Route to High-Performance Solar Cell Production? Joule 2017, 1, 431–442.
98. Longo, G.; Gil-Escrig, L.; Degen, M.J.; Sessolo, M.; Bolink, H.J. Perovskite solar cells prepared by flash evaporation. Chem. Commun. 2015, 51, 7376–7378.
99. Rong, Y.; Hu, Y.; Mei, A.; Tan, H.; Saidaminov, M.I.; Seok, S., II; McGehee, M.D.; Sargent, E.H.; Han, H. Challenges for commercializing perovskite solar cells. Science 2018, 80, 361.
100. Ke, W.; Zhao, D.; Cimaroli, A.J.; Grice, C.R.; Qin, P.; Liu, Q.; Xiong, L.; Yan, Y.; Fang, G. Effects of annealing temperature of tin oxide electron selective layers on the performance of perovskite solar cells. J. Mater. Chem. A 2015, 3, 24163–24168.
101. Gao, L.L.; Li, C.X.; Li, C.J.; Yang, G.J. Large-area high-efficiency perovskite solar cells based on perovskite films dried by the multi-flow air knife method in air. J. Mater. Chem. A 2017, 5, 1548–1557.